Diffusion through Bifurcations in Oscillating Nano- and Microscale Contacts: Fundamentals and Applications

Ming Ma,[1] Igor M. Sokolov,[2] Wen Wang,[3,4] Alexander E. Filippov,[5] Quanshui Zheng,[3,4] and Michael Urbakh[1,*]

[1]*School of Chemistry, Tel Aviv University, 69978 Tel Aviv, Israel*
[2]*Institut für Physik, Humboldt-Universität zu Berlin, Newtonstrasse 15, D-12489 Berlin, Germany*
[3]*Department of Engineering Mechanics, Tsinghua University, Beijing 100084, China*
[4]*Center for Nano and Micro Mechanics, Tsinghua University, Beijing 100084, China*
[5]*Donetsk Institute for Physics and Engineering of NASU, 83114 Donetsk, Ukraine*

(Received 4 May 2015; revised manuscript received 15 July 2015; published 21 August 2015)

It has long been recognized that the diffusion of adsorbed molecules and clusters is the key controlling factor in most dynamical processes occurring on surfaces and in nanoscale-confined spaces. The ability to manipulate diffusion is essential for achieving efficient transport in nano- and microstructures and for many other applications. Through simulations and experiments, we found that under the influence of mechanical oscillations, the diffusion coefficient in nanoscale-confined regions can be greatly enhanced. This effect occurs due to bifurcations of particle trajectories caused by the reconstruction of the energy landscape during oscillations. We derive a parameter-free analytical model for the enhanced diffusion that is in excellent agreement with results of our numerical simulations. The oscillation-induced enhancement of diffusion may have interesting and promising applications in such areas as directed molecular transport, sorting of particles, and tribology. Here, our findings have been applied to studies of mechanical cleaning of surfaces from contamination. Through both experiments and simulations, we have shown that using an oscillating slider, one can significantly reduce the concentration of contaminants in a confined region, which is crucial for achieving superlow friction.

DOI: 10.1103/PhysRevX.5.031020

Subject Areas: Materials Science, Nonlinear Dynamics, Statistical Physics

I. INTRODUCTION

Studies of the diffusive properties of adsorbates are of broad scientific and technological importance in areas ranging from chemical kinetics [1,2] and surface nanostructuring [3,4] to molecular sorting [5–7], directed transport [8,9], and tribology [10,11]. At surfaces, the molecular diffusion is usually reduced compared to that in gas or liquid phases because of the potential energy landscape impeding molecular motion. The ability to enhance or, more generally, to manipulate diffusion at the nanoscale presents a great challenge for both fundamental studies and applications. It has been theoretically demonstrated that significant enhancement of diffusion can be achieved by applying external time-dependent forces with zero mean [12,13] or through temporal modulations of surface potential [14,15]. These effects have been observed for colloidal particles in a periodic potential whose potential barriers are subjected to temporal oscillations [16] and for paramagnetic particles moving on a magnetically structured substrate and subjected to a periodic forcing of an external magnetic field [17]. However, it seems impossible to implement these ideas under a strict size confinement typical for nanodevices, which leaves very limited access to interfere with the system in order to be able to enhance diffusion.

In this paper, we investigate the mechanism of diffusion of adsorbed molecules confined between oscillating surfaces that is a common configuration for tribology. Through both modeling and explicit molecular dynamics simulations, we find that in applying mechanical oscillations, the diffusion coefficient in a nanoscale-confined region can be greatly enhanced compared to the diffusion coefficient on immobile surfaces. The giant enhancement of diffusion occurs due to bifurcations of particle trajectories caused by the reconstruction of the energy landscape during oscillations. An analytical model has been derived that describes quantitatively dependencies of the diffusion coefficient on frequency and amplitude of oscillation and on temperature.

We have studied experimentally a process of mechanical cleaning of surfaces using an oscillating slider and found that enhancement of diffusion in the confined region leads to significant reduction of contaminant concentration, which is difficult to achieve by conventional cleaning

*urbakh@post.tau.ac.il

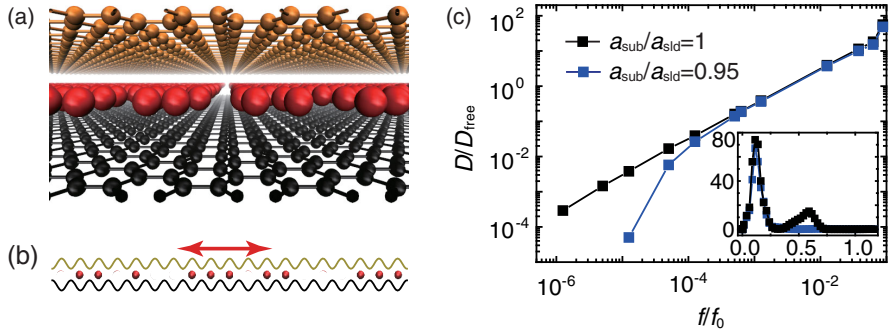

FIG. 1. Schematics of the studied systems and enhanced diffusion. (a) Schematic sketch of experimental configuration and (b) the model geometry, where red spheres represent particles embedded between two surfaces shown as black and yellow spheres (curves). The arrows in (b) indicate the directions of oscillations. (c) Dependence of normalized diffusion coefficient D/D_{free} on frequency of oscillations f/f_0 calculated for commensurate ($a_{\mathrm{sub}}/a_{\mathrm{sld}} = 1$) and incommensurate ($a_{\mathrm{sub}}/a_{\mathrm{sld}} = 0.95$) surfaces, with $D_{\mathrm{free}} = k_B T/\eta_{\mathrm{sub}}$ being the free diffusion coefficient and the oscillation amplitude A being $A/a_{\mathrm{sld}} = 2$. The inset shows this dependence in the high-frequency range.

techniques. The experimental observations have been compared with the predictions of simulations.

II. THEORETICAL MODEL

In order to mimic the commonly used experimental configuration depicted in Fig. 1(a), we consider a one-dimensional model that includes two rigid plates and adsorbed particles of mass m embedded between them, as shown in Fig. 1(b). The top plate (slider) oscillates harmonically with a frequency f and amplitude A, while the bottom plate (substrate) is fixed. The motion of the ith adsorbed particle is governed by the following Langevin equations

$$m\ddot{x}_i = F_i^{\mathrm{sub}} + F_i^{\mathrm{sld}} - \eta_{\mathrm{sub}}\dot{x}_i - \eta_{\mathrm{sld}}(\dot{x}_i - v_{\mathrm{sld}}) + F_i^{a-a} + \gamma_i(t), \tag{1}$$

where x_i is the coordinate of the ith particle; $F_i^{\mathrm{sub}} = U_{\mathrm{sub}}(2\pi/a_{\mathrm{sub}})\cos(2\pi x_i/a_{\mathrm{sub}})$ and $F_i^{\mathrm{sld}} = U_{\mathrm{sld}}(2\pi/a_{\mathrm{sld}})\times\cos[(2\pi/a_{\mathrm{sld}})(x_i - X_{\mathrm{sld}})]$ are the forces describing the particle-substrate and particle-slider interactions, respectively; a_{sub} and a_{sld} are the spatial periodicities of the substrate and slider; $X_{\mathrm{sld}} = A\sin(2\pi f t)$ is the center-of-mass coordinate of the slider; F_i^{a-a} is the force describing interparticle interactions, which are modeled by the Gaussian repulsive potential $U^{a-a}(r) = U_0^{a-a}\exp[-(r/b)^2]$ with r being the interparticle distance; η_{sub} and η_{sld} are the damping constants responsible for the dissipation of the particle kinetic energy to the substrate and slider; and $\gamma_i(t)$ is the random force representing thermal noise and satisfying the fluctuation-dissipation relation. The results presented in the paper have been obtained choosing the parameters of interparticle interactions as $U_0^{a-a} = 0.2U_{\mathrm{sub}}$ and $b = (a_{\mathrm{sub}}/2\pi)$. Similar results have also been obtained for Lennard-Jones interactions between particles (see the Supplemental Material) and for the Gaussian repulsive potential with different values of parameters.

In simulations, before applying oscillations to the slider, the adsorbates are uniformly distributed on the substrate with a given surface concentration $N_{\mathrm{ads}}/N_{\mathrm{sub}} = 0.5$, where N_{sub} is the number of substrate atoms, and the system is equilibrated at finite temperature T with the Langevin thermostat. Then, the oscillations are applied and the simulations are performed during 200 periods. A broad range of frequencies spanning over 6 orders of magnitude has been studied: $1.26\times10^{-6} < f/f_0 < 1.24$, where $f_0 = (1/a_{\mathrm{sub}})\sqrt{(U_{\mathrm{sub}}/m)}$ is the intrinsic frequency for small oscillations at the minima of the substrate potential. The velocity Verlet method has been used to integrate the equations of motion. There is ample evidence from the field of atomic and molecular vibrations and diffusion that the molecular motion on this small scale is close to critically damped [18,19]. Therefore, most of the results presented below have been obtained for the values of the damping coefficient, which are critical with respect to the interaction between the particles and surfaces $\eta_{\mathrm{sub}} = 4\pi\sqrt{U_{\mathrm{sub}}m}/a_{\mathrm{sub}}$ and $\eta_{\mathrm{sld}} = 4\pi\sqrt{U_{\mathrm{sld}}m}/a_{\mathrm{sld}}$. These values of the damping coefficient correspond to the transition between the oscillatory and aperiodic behaviors of a single particle in a single potential well. The simulations performed in the overdamped regime of motion lead to similar conclusions.

III. ENHANCED DIFFUSION

First, we present in Fig. 1(c) results obtained for low temperature $T = 0.01U_{\mathrm{sub}}/k_B$. Both commensurate ($a_{\mathrm{sld}}/a_{\mathrm{sub}} = 1$) and incommensurate surfaces with the same potential corrugation $U_{\mathrm{sld}} = U_{\mathrm{sub}}$ have been studied, and in the latter case, the misfit $\varepsilon = (a_{\mathrm{sld}} - a_{\mathrm{sub}})/a_{\mathrm{sld}}$ is changed from 0.025 to 0.2. In all cases, we find a giant enhancement of diffusion coefficient induced by oscillations. In Fig. 1(c),

we present the diffusion coefficient normalized to the diffusion coefficient of free particles $D_{\mathrm{free}} = k_B T/\eta_{\mathrm{sub}}$ (in the absence of interaction with a surface). The diffusion coefficient at a fixed surface can be estimated as $D_{\mathrm{free}}\exp(-U_{\mathrm{sub}}/k_B T)$ and, for instance, with $T = 0.05U_{\mathrm{sub}}/k_B$ it is 8 orders of magnitude lower than D_{free}. Under these conditions, the oscillation-induced diffusion coefficient may be more than 10 orders of magnitude higher than the diffusion coefficient at the substrate surface in the absence of oscillations.

For both commensurate and incommensurate contacts, a nonlinear dependence of D on f has been found at high frequencies ($f/f_0 > 0.1$), as shown in the inset in Fig. 1(c). This effect is similar to the previously discussed giant enhancement of diffusion under the action of external time-dependent force with zero mean [12,13,20] or vibrations of substrate surface [21]. Here, we focus on another regime of diffusion that emerges at low frequencies $f/f_0 < 0.06$. This regime, as we show below, is of experimental relevance. In this regime, for commensurate surfaces, D depends linearly on f for all frequencies studied in the simulations [black squares in Fig. 1(c)]. For incommensurate surfaces in the intermediate range of frequencies (e.g., $6.28 \times 10^{-4} < f/f_0 < 0.06$ for $\varepsilon = 0.05$), D exhibits the same linear dependence on f as for commensurate surfaces; however, for lower frequencies, $D(f)$ deviates from linearity, becoming smaller than that for the commensurate surfaces. The threshold frequency at which $D(f)$ starts to deviate from the linear law increases with increasing misfit ε. It should be noted that linear variation of D with f has been previously found in simulations of diffusion in a periodic potential with temporally changing amplitude [14,15]. The prediction of oscillation-induced enhancement of diffusion of particles confined between incommensurate surfaces has been confirmed qualitatively in our experiments on mechanical cleaning, which are discussed in the next section.

To understand the mechanism of diffusion leading to the linear dependence of D on f that covers a wide frequency range, we present in Fig. 2 the trajectories of adsorbed particles and time evolution of potential profiles calculated for both commensurate and incommensurate surfaces during two periods of oscillations. As shown in Fig. 2(a), bringing the trajectories to a common start point, for the commensurate surfaces, we find a pattern that results from perfect multiple bifurcations of trajectories, which occur under the influence of the oscillations. At $t = 0$, all particles are located in the minima of potential created by the confining surfaces [Fig. 2(c)]. When the slider starts to oscillate, the position of the potential minimum changes with time. At low frequencies, the particles follow the position of the minimum adiabatically as shown in Fig. 2(c) before the first bifurcation point. As the oscillation proceeds, at a certain time, the minimum of potential energy [indicated as blue regions in Fig. 2(c)] transforms into the maximum [red regions in Fig. 2(c)] and two new potential

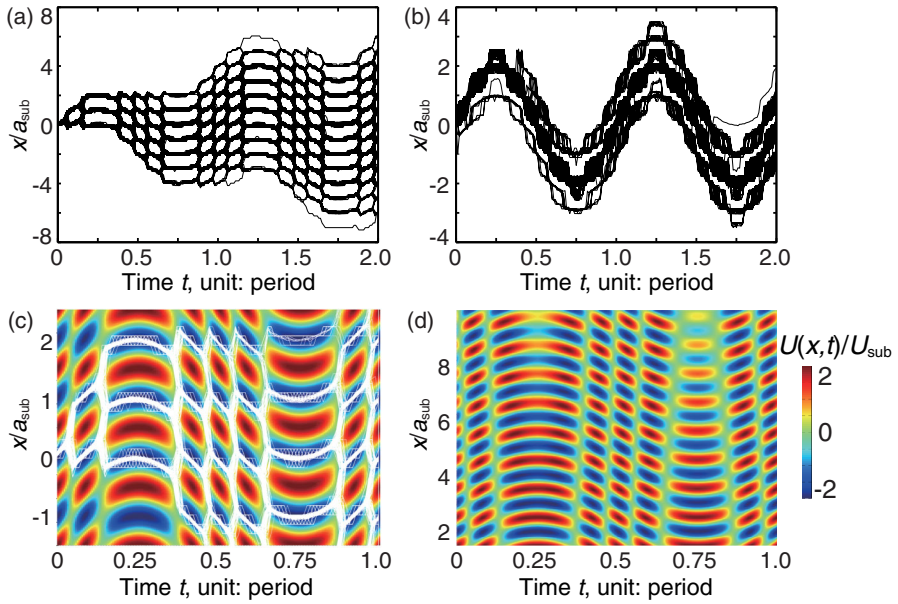

FIG. 2. Mechanisms of enhanced diffusion. (a),(b) Trajectories of adsorbates calculated for commensurate surfaces oscillating with frequency $f/f_0 = 1.26 \times 10^{-2}$ and for incommensurate surfaces ($a_{\mathrm{sub}}/a_{\mathrm{sld}} = 0.95$) with $f/f_0 = 1.26 \times 10^{-5}$, respectively. The oscillation amplitude is $A = 2a_{\mathrm{sld}}$. The time interval in (a) and (b) corresponds to two periods of oscillations. Note that different scales of the Y axis are used for better visualization. (c),(d) Time evolution of the potential energy experienced by particles $U(x, t)$ for commensurate and incommensurate ($\varepsilon = 0.05$) surfaces, respectively. Blue and red regions correspond to potential minima and maxima, respectively. The color bar is shown to the right of (d). The time interval in (c) and (d) corresponds to one period of oscillations. White curves in (c) show trajectories of adsorbates.

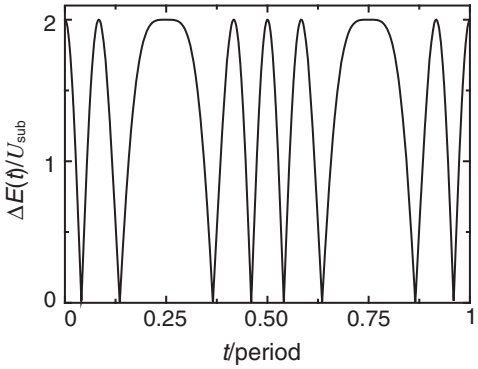

FIG. 3. Variation of potential energy barriers separating the neighboring minima in the particle-substrate energy landscape with time during one period of oscillations with the amplitude equal to $A = 2a$. The results are for commensurate surfaces.

minima appear simultaneously at a distance of $a_{sub}/2$ to the left and right of the former minimum. The variation of potential energy barriers separating the neighboring minima in the particle-substrate energy landscape with time during one period of oscillations is shown in Fig. 3.

We can introduce a "landscape reconstruction time" Δt_r that is a time interval during which the barriers separating neighboring minima are very low, of the order of k_BT or even smaller, as indicated by green regions in Fig. 2(c). The time Δt_r is proportional to the temporal period of oscillations and depends on k_BT. During the landscape reconstruction time, the particles leave the former minimum and jump to the new neighboring minima with equal probabilities, since for commensurate surfaces, the energy landscape is symmetric with respect to the position of the former minimum. After this bifurcation transition, the positions of new potential minima change continuously with time, and the barrier heights separating minima become much larger than k_BT, thus trapping particles until the next transition. In this quasistatic regime, the motion of particles can be described as a random walk. At each bifurcation point, the particles jump randomly to one of the two neighboring minima with the same probabilities, and the jump length equals to half of the substrate period. Correspondingly, the diffusion coefficient can be written as [22]

$$D = (a_{sub}/2)^2/2\Delta t = a_{sub}Af/2, \tag{2}$$

where $\Delta t = 1/fN_b$ is the average time between bifurcations and $N_b = 4A/a_{sub}$ is the number of bifurcations per period of oscillations. In the quasistatic regime, which spans over 5 orders of magnitude of f, this equation is in excellent agreement with the results of numerical simulations, as shown in Fig. 5(a). Equation (2) also demonstrates that in the quasistatic regime, D is proportional to the amplitude of oscillations that is confirmed by numerical simulations. For $A = 1$ μm, $f = 10$ kHz, and $a_{sub} = 0.2$ nm, we get $D = 1 \times 10^{-8}$ cm^2/s that is more than 10 orders of magnitude larger than the diffusion coefficient at the fixed surface calculated for $U_{sub} = 0.1$ eV and $m \sim 100$ atomic mass unit.

For incommensurate surfaces [see Fig. 1(c)], $D(f)$ changes linearly in the intermediate frequency range; however, it deviates from the linearity for frequencies lower than $f/f_0 = 6.28 \times 10^{-5}$. Figure 2(b), showing the trajectories of the particles at low frequency $f/f_0 = 1.26 \times 10^{-5}$, exhibits an asymmetric splitting of particles rather than the symmetric one observed for the commensurate surfaces. This behavior can be understood comparing the time evolution of the energy landscapes for commensurate and incommensurate surfaces shown in Figs. 2(c) and 2(d). The major difference between the two maps shown in Figs. 2(c) and 2(d) is that during the landscape reconstruction time Δt_r, the energy profile for the commensurate contact is symmetric with respect to the position of the former minimum, while for the incommensurate one, that is not the case. This effect is manifested by the inclination of green domains in Fig. 2(d), which represents the potential energy profile during Δt_r. Thus, for incommensurate surfaces, there is small bias force F_b acting toward one of the two newly appearing neighboring minima. The force-induced (deterministic) and diffusive (random) displacements of particles during the landscape reconstruction time Δt_r can be estimated as $\Delta x_b \sim F_b\Delta t_r^2/(2m)$ and $\Delta x_d \approx \sqrt{2D_{free}\Delta t_r}$, respectively. If the oscillations are not too slow, Δx_b is much smaller than Δx_d simply because for small Δt_r, the square root wins. The diffusive displacement is symmetric and moves the particles to new minima with equal probabilities. In this range of frequencies, the diffusion coefficient for incommensurate surfaces scales linearly with f and coincides with D for commensurate surfaces. When the period of oscillations gets too long, Δt_r gets large, the drift ($\Delta x_b \sim \Delta t_r^2$) starts to win over the diffusion ($\Delta x_d \sim \sqrt{\Delta t_r}$), and the particles go with the overwhelming probability either left or right. As a result, the trajectories get more and more deterministic, resulting in a smaller D compared to that for the commensurate surfaces.

The simulations discussed above have been performed for the critical values of damping coefficients. However, it is important to understand what would happen for higher damping, which is characteristic for experiments with a colloidal system diffusing over laser-generated periodic potentials [23] that may provide direct evidence of the predicted mechanism of the enhancement of diffusion. For commensurate surfaces, in the range of frequencies, where $D(f)$ changes linearly with f under critical damping, the simulations performed for the overdamped conditions show the same results as for the critical damping [see Fig. 4(a)]. Figure 4(b) shows that for incommensurate contacts, the range of frequencies, where we found a linear dependence of D on f, becomes broader, extending to lower frequencies compared to the case of the critical damping. The latter

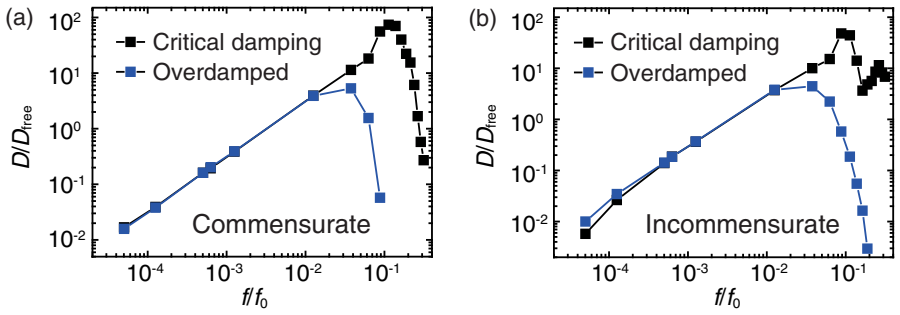

FIG. 4. Diffusion coefficients with different damping coefficients for adsorbates confined between the (a) commensurate and (b) incommensurate ($a_{sub}/a_{sld} = 0.95$) surfaces. The oscillation amplitude is $A = 2a_{sld}$. The damping coefficients for the overdamped case are two times larger than their values for the critical damping.

is explained by the fact that the force-induced (deterministic) displacements of particles during the landscape reconstruction time that lead to the deviation from the linear law become less significant under the overdamped conditions, and the symmetric diffusive displacements dominate in a broader range of frequencies.

Figure 4 also shows that at high frequencies, the results obtained for higher damping deviate from the linear relation found for the critical damping. At these frequencies, the viscous force acting on the particles $\eta_{sub}\dot{x}_i - \eta_{sld}(\dot{x}_i - v_{sld})$ becomes of the same order or even larger than the potential forces and the bifurcation mechanism of diffusion stops working. The limiting frequency above which this mechanism fails can be estimated by comparing the amplitude of the potential force with that of the viscous force. This gives $f_{lim} = (U_{sub}/a_{sld})/(A\eta_{sub})$, showing that the limiting frequency decreases with increase of damping. In our cases, f_{lim}/f_0 equals to 0.16 for critical damping and 0.05 for overdamped particles, which are in the excellent agreement with the numerical results for both commensurate and incommensurate surfaces (Fig. 4).

Equation (2) for the oscillation-induced diffusion coefficient has been derived for noninteracting adsorbed particles. The bifurcation mechanism of oscillation-induced enhancement of diffusion is expected to work when the concentration of particles is low enough and they do not cluster. Under these conditions, the exact form of the potential does not play any role. However, our simulations show that in the considered range of parameters, the effect of soft Gaussian repulsion between the particles on the diffusion coefficient is negligible even for high surface concentration $N_{ads}/N_{sub} = 0.5$. The exact values of the parameters of the Gaussian potential only slightly influence the magnitude of the oscillation-induced diffusion coefficient. Unlike hard spheres or Lennard-Jones potentials, the Gaussian repulsive potential allows for the possibility that the particles can pass through each other even in 1D systems. This enables us within the 1D model considered here to mimic 2D dynamics, where, contrary to 1D, bypassing is possible. We have found that the predicted mechanism of enhancement of diffusion through bifurcation works also for the Lennard-Jones interaction between particles, and at low oscillation frequencies, which are discussed in this work, the oscillation-induced diffusion coefficient exhibits a linear dependence on f [24]. However, in this case, the values of the diffusion coefficient decrease with increase of the particle concentration, indicating that collective behavior of the adsorbates (e.g., clustering) plays a role.

So far, we have discussed oscillation-induced diffusion at low temperatures where D is completely determined by the bifurcation mechanism. For higher temperatures, the diffusion coefficient as a function of f exhibits a crossover from the linear dependence for intermediate range of frequencies, where it coincides with $D(f)$ for low temperature, to a constant at lower frequencies. In Fig. 4(a), we show $D(f)$ calculated for commensurate surfaces at temperature $T = 0.2U_{sub}/k_B$ that for U_{sub} of the order of 0.1 eV corresponds to room temperature. Here, in the low-frequency limit, the diffusion coefficient is three orders higher than the diffusion coefficient on immobile surfaces at the same temperature. When the temperature is raised, the possibility of thermally activated jumps above the barrier appears, and at high temperatures, such thermally activated jumps dominate the diffusion. The particle trajectories in this regime are shown in the Supplemental Material [24]. In this case, the mean-squared diffusive displacements of particles during the landscape reconstruction time increase with T, and at low frequencies, it becomes larger than the substrate period. Then, $(\Delta x_d)^2 \sim \Delta t_r \sim 1/f$, and considering that the time between bifurcations scales as $\Delta t = 1/fN_b$, we find that $D(f)$ levels off at low frequencies, as shown in Fig. 4(a). At intermediate frequencies, the particles are transferred only to the closest neighboring minima, and $D(f)$ is described by Eq. (2) exhibiting a linear dependence on f.

Based on the mechanisms revealed above, we have derived a parameter-free analytical model for $D(f)$ that considers the whole process as a superposition of two random walks, one described by the splitting of trajectories at the bifurcation points and the other corresponding to jumps between adjacent minima of the potential when

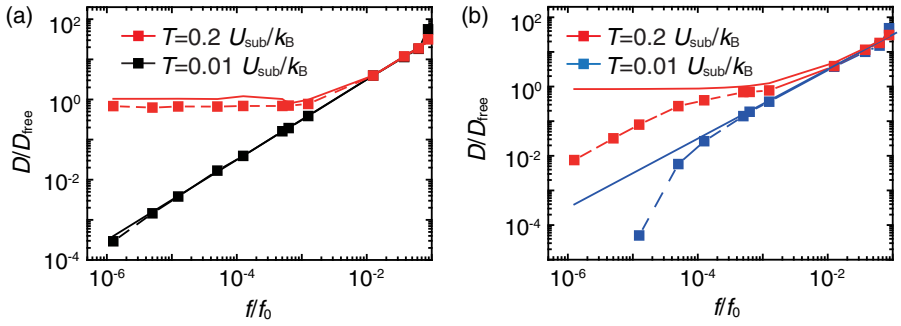

FIG. 5. Diffusion coefficient as a function of frequency at $T = 0.01U_{sub}/k_B$ and $T = 0.2U_{sub}/k_B$ for (a) commensurate and (b) incommensurate $\varepsilon = 0.05$ surfaces. Square dots connected by dashed lines are numerical results, and curves show theoretical results. The oscillation amplitude is $A = 2a_{sld}$. The normalization coefficient D_{free} corresponds to $T = 0.01U_{sub}/k_B$.

the barrier does not vanish. The mean-squared displacement in both walks sum up, and so do the diffusion coefficients. The overall effective diffusion coefficient is $D_{eff} = D_{bif} + D_{act}$. The diffusion coefficient for the bifurcation process is given by Eq. (2), and the diffusion coefficient D_{act} due to the thermally activated processes can be evaluated as the mean over the oscillation period of instantaneous coefficients of diffusion as obtained through the activation mechanism $D_{act} = (1/T)\int_0^T D(t)dt$, where the instantaneous diffusion coefficient $D(t)$ is given by the Arrhenius formula $D = (k_BT/\eta)\exp(-\Delta E/k_BT)$. Here, ΔE is the height of the energy barrier at time t, as shown in Fig. 3. This parameter-free analytical model for $D(f)$ covers both the linear and the frequency-independent behaviors, and the transition between them. As shown in Fig. 5(a), it agrees well with the numerical results. The validity of the analytical model has also been proven for a wide range of temperatures $10^{-2}U_{sld}/k_B \leq T \leq 0.4U_{sld}/k_B$ [24].

In Fig. 5(b), we show $D(f)$ for incommensurate surfaces ($\varepsilon = 0.05$, as an example) calculated for two temperatures $T = 0.01U_{sub}/k_B$ and $T = 0.2U_{sub}/k_B$. In the linear regime of variation of D with f, the theoretical model (curves) still shows good agreement with numerical results. For lower frequencies, the model overestimates the diffusion coefficient for incommensurate surfaces. As we discussed above, in this case, the asymmetry of the potential profile during the landscape reconstruction time leads to the asymmetric splitting of particle trajectories, resulting in smaller diffusion coefficients. With the increase of the difference between the properties of confining surfaces described by the parameters a_{sld} and a_{sub}, U_{sld} and U_{sub}, and η_{sld} and η_{sub}, the oscillation-induced diffusion coefficient decreases.

IV. MECHANICAL CLEANING OF SURFACES

The enhancement of diffusion in oscillating contacts discussed above may have interesting and promising applications in such areas as directed molecular transport [8,9], sorting of particles [5–7], and tribology [10,11]. Here, we consider the manifestation of this effect in a process of mechanical cleaning of surfaces from contamination using an oscillating slider (mechanical wiping). *In situ* cleaning of tribological contacts is crucial for achievement of the superlow-friction state (superlubricity), which may be destroyed due to the presence of contaminations between the surfaces [25,26]. Recently, it has been experimentally demonstrated that mechanical wiping of graphite surfaces using a graphite microflake may drastically reduce the amount of contaminations on surfaces [27]. Using this approach, individual surface areas can be cleaned selectively, which is difficult to achieve with any conventional cleaning technique.

In experiments on cleaning via mechanical oscillation illustrated in Figs. 6(a)–(c), we use graphite mesa as the substrate and slider. First, the graphite mesas are prepared [Fig. 6(a)]; then, the surfaces are exposed to air for several minutes, during which contaminants are adsorbed [Fig. 6(b)], and after that, the cover of the right mesa is transferred to the top of the left one, the oscillations are applied to the slider, and friction measurements are performed [Fig. 6(c)]. Details of the sample preparation and friction force measurements are provided in Appendixes A and B, respectively. Two sets of experiments with oscillation amplitudes $A \sim 0.08L$ and $A \sim 1.0L$, where $L \sim 3$ μm is the size of the slider, have been performed. A reduction of the amount of contaminants confined between surfaces $N^{conf}(t)$ with the number of oscillation periods has been measured indirectly through the decrease of the kinetic friction force, assuming that for incommensurate contacts, the friction is proportional to the number of embedded particles (see the Supplemental Material [24] for details). As shown in Figs. 6(e) and 6(f), a gradual reduction of contaminants with a characteristic time scale of tens of periods has been observed, indicating that the mechanical cleaning is a diffusion-limited process.

In simulations of mechanical cleaning, we slightly modify the system used above for calculations of diffusion in order to include the finite size of the slider and properly describe interactions of adsorbed particles with the slider edges. The slider and substrate are modeled as 1D arrays

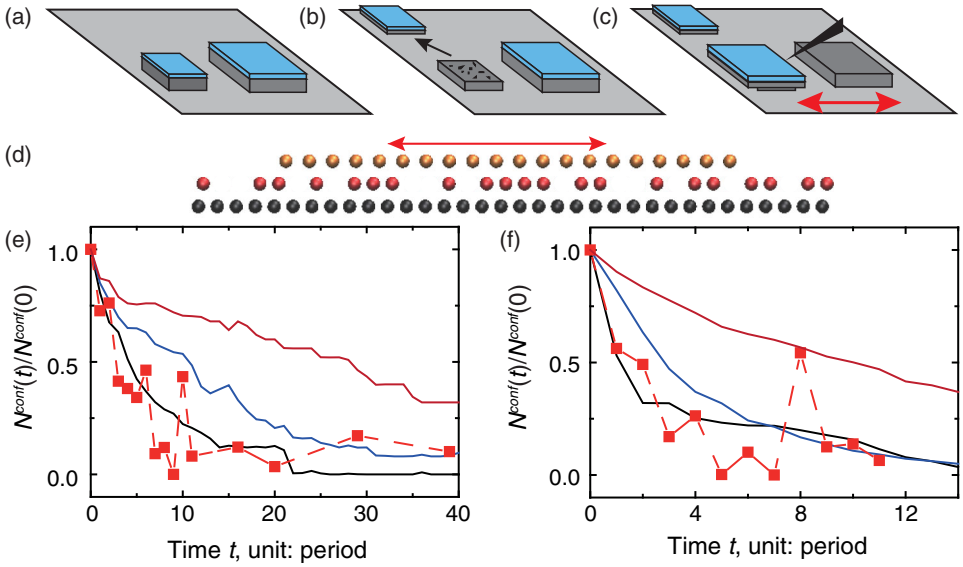

FIG. 6. Mechanical cleaning of surfaces. (a)–(c) Schematic representation of the experimental procedure including (a) preparation of graphite mesas, (b) adsorption of contaminants, and (c) transferring of the cover of the right mesa to the top of the left one and mechanical cleaning. The top parts in blue are SiO_2, and the rest in gray are graphite mesas. The black triangle stands for the tip of the microforce sensing probe, and the red arrows indicate the direction of the oscillation of the substrate. (d) Schematic sketch of the model used to simulate the cleaning process via mechanical oscillation. Golden spheres represent the slider surface that oscillates as indicated by the arrows, red spheres show adsorbed particles, which initially are uniformly distributed, and black spheres depict the substrate. (e), (f) Comparison between the values of $N^{\mathrm{conf}}(t)/N^{\mathrm{conf}}(0)$ measured in experiments (square symbols connected by dashed lines) and calculated in simulations (curves) for small ($A \sim 0.1L$, where L is the size of the slider) and large amplitudes ($A \sim 1.0L$) of oscillations, respectively. In (e), the curves from top to bottom have been calculated for $f/f_0 = 1.26 \times 10^{-2}$, 5.03×10^{-5}, and 1.26×10^{-5}, respectively. In (f), the curves from top to bottom correspond to $f/f_0 = 1.26 \times 10^{-2}$, 1.26×10^{-3}, and 5.03×10^{-5}, respectively. Simulations have been performed for incommensurate surfaces with $a_{\mathrm{sld}}/a_{\mathrm{sub}} = (1+\sqrt{5})/2$ and $T = 0.2U_{\mathrm{sub}}/k_B$.

including N_{sld} and N_{sub} atoms with interatomic distance a_{sub} and a_{sld}, respectively [see Fig. 6(d) for a schematic sketch of the system]. The interactions between the adsorbed particles and surface atoms are described by Lennard-Jones potentials with parameters chosen in such a way that the particles embedded between surfaces and located away from the slider edges experience the same periodic potential as in diffusion simulations. However, at the edges of the slider, the energy barriers are higher than in the confinement.

For systems illustrated in Fig. 6(d), in order to characterize quantitatively the cleaning process, we calculate the normalized number of adsorbates in the confined region as a function of time $p(t) = N^{\mathrm{conf}}(t)/N^{\mathrm{conf}}(0)$. Averaging $p(t)$ over a number of realizations gives a survival probability for the particles to stay in the confined region. As we show below, $p(t)$ depends on both frequency and amplitude of oscillations. Following the experimental procedure, we perform simulations for both small $A \sim 0.1L$ and large $A \sim 1.05L$ amplitudes of oscillations, where $L = N_{\mathrm{sld}}a_{\mathrm{sld}}$ is the slider length. For not too short times, $N^{\mathrm{conf}}(t)/N^{\mathrm{conf}}(0)$ is equal to $\exp(-t/\tau)$, where $\tau = 1/\lambda D$, D is the diffusion coefficient in the confined region, and $\lambda > 0$ is a parameter depending on boundary conditions at the slider edges and the slider length [28]. In the case of absorbing boundaries, for which the particles are removed from the confinement as they reach the slider edges, $\lambda = \pi^2/(L+2A)^2$, while for reflecting boundaries, $N^{\mathrm{conf}}(t)/N^{\mathrm{conf}}(0) = 1$ and $\lambda = 0$. Modeling the cleaning experiments, we have to consider that the particles may leave the confined region. The simulations show that particles leaving the confined region are partially reflected by the slider edges, and the partially absorbing boundary conditions should be applied, for which the parameter λ lies between two limiting values corresponding to absorbing and reflecting boundaries. Thus, the cleaning efficiency $1 - p(t)$ is determined by both the diffusion coefficient in the confinement and the boundary conditions at the slider edges.

It is instructive to present the results of cleaning simulations as a function of number of oscillation periods $t_n = tf$, as shown in Figs. 6(e) and 6(f). Measuring time in the number of periods can be used to compare the results at different frequencies and with the ones of experiment. Then, in the frequency range for which the diffusion coefficient changes linearly with f, we get the equation $p(t_n) = \exp(-t_n\lambda A a_{\mathrm{sub}}/2)$, where λ is the only frequency-dependent parameter. Our simulations show that the probability of a particle to be reflected by the slider edges increases with f, and thereby λ decreases with increasing f. Thus, for a given number of periods, the cleaning is more efficient (the survival probability

becomes lower) for lower frequencies, as shown in Figs. 6(e) and 6(f). The same conclusion is correct for lower frequencies, where $D(f)$ is a constant, and $p(t_n)$ changes as $p(t_n) = 1 - \exp(-t_n \lambda D/f)$.

In Figs. 6(f), we compare the results of our measurements with the numerical results obtained for incommensurate surfaces with $a_{\mathrm{sld}}/a_{\mathrm{sub}} = (1+\sqrt{5})/2$ corresponding to the golden ratio and temperature $T = 0.2U_{\mathrm{sld}}/k_B$. The golden ratio represents the "most irrational" incommensurability between contacting surfaces, which results in superlow friction in the absence of contaminants [29]. For both small and large amplitudes of oscillations, the results of simulations approach the experimental data as frequency decreases. A higher efficiency of cleaning, which has been found for large oscillation amplitudes both in experiments and in simulations, results from the effect of pushing of adsorbed particles outside the confined region by the slider edges, which speeds up the process [24]. The effect of pushing is less significant for the smaller amplitudes for which the enhanced diffusion completely dominates the cleaning process.

Our model gives a clear qualitative description of the experiments on cleaning via mechanical oscillations; however, at the present stage, it cannot be pushed to give quantitative predictions, since the simulation results depend not only on the frequency but also on the unknown parameters of the experiment, such as particle-substrate interactions, boundary conditions, etc. Direct quantitative evidence of the predicted effect can be provided by experiments with two-dimensional colloidal systems diffusing over laser-generated periodic potentials [23].

V. CONCLUSIONS

To summarize, we have found a significant enhancement of diffusion coefficients in nanoscale confinement under the influence of mechanical oscillations. The giant enhancement of diffusion occurs due to bifurcations of particle trajectories caused by the reconstruction of the energy landscape during oscillations. The oscillation-induced enhancement of diffusion may have interesting and promising applications in such areas as directed molecular transport, sorting of particles, and tribology. Here, our findings have been applied to studies of the mechanical cleaning of surfaces, which demonstrated that enhancement of diffusion leads to a significant reduction of contaminant concentration in the confined region.

ACKNOWLEDGMENTS

M. M. acknowledges financial support from a fellowship program for outstanding postdoctoral researchers from China and India in Israeli Universities. I. M. S. and M. U. acknowledge the financial support of the TAU-HUB program "Biological and Soft Matter Physics," M. U. acknowledges the financial support of the Israel Science Foundation, Grant No. 1316/13, Q. Z. and M. U. acknowledge the support of XIN center, Tel Aviv - Tsinghua Universities, and M. M., A. E. F., and M. U. acknowledge the support of COST Action MP1303.

APPENDIX A: SAMPLE PREPARATION

Microscale graphite mesa samples are used to build the systems (see the Supplemental Material [24] for details of sample preparation). First, samples of different sizes (3 μm for small samples and 10 μm for big samples), which exhibit self-retraction, have been identified. These self-retraction samples have flat surfaces and exhibit superlow friction (superlubricity) due to incommensurability of contacting surfaces [30,31]. We use a tungsten tip to push the upper part of the small graphite mesa away, and the cleaved surfaces are exposed to air at a temperature of 23 °C and 10% humidity for several minutes. During this time, molecules and probably larger contaminants have been adsorbed on surfaces, as indicated in Fig. 6(b). Finally, we use the tungsten tip to transfer the upper part of the large sample to cover the small sample [Fig. 6(c)] and leave the sample for approximately 15 minutes before the friction force measurements with the oscillating slider are started.

APPENDIX B: FRICTION FORCE MEASUREMENT

For the friction force measurement, we employ a microforce sensing probe FemtoTools FT-S100 with force resolution of 5 nN and a bandwidth of up to 8 kHz; see Fig. 6(c). The microforce sensing probe is calibrated *in situ* using the method reported in Ref. [32]. The sample is placed on a three-dimensional platform with the help of which the speed and displacement could be controlled precisely. Measurements of friction force are performed by bringing the tip of the microforce sensing probe into contact with the SiO_2 layer grown on the top surface of the highly oriented pyrolytic graphite sample by plasma-enhanced chemical vapor deposition, and by moving the platform at a constant speed of 25 nm/s while keeping the microforce sensing probe fixed [Fig. 6(c)]. A typical loading displacement was about 500 nm. After measuring the friction, the sample is pushed back to its initial position with speed of 1 μm/s, and another cycle of measurements is started.

[1] I. M. Sokolov, J. Klafter, and A. Blumen, *Fractional Kinetics*, Phys. Today **55**, No. 11, 48 (2002).

[2] O. Benichou, C. Chevalier, J. Klafter, B. Meyer, and R. Voituriez, *Geometry-Controlled Kinetics*, Nat. Chem. **2**, 472 (2010).

[3] G. S. Parkinson, Z. Novotny, G. Argentero, M. Schmid, J. Pavelec, R. Kosak, P. Blaha, and U. Diebold, *Carbon*

Monoxide-Induced Adatom Sintering in a Pd-Fe_3O_4 *Model Catalyst*, Nat. Mater. **12**, 724 (2013).

[4] T. Mitsui, M. K. Rose, E. Fomin, D. F. Ogletree, and M. Salmeron, *Water Diffusion and Clustering on Pd(111)*, Science **297**, 1850 (2002).

[5] J. K. Holt, H. G. Park, Y. M. Wang, M. Stadermann, A. B. Artyukhin, C. P. Grigoropoulos, A. Noy, and O. Bakajin, *Fast Mass Transport Through Sub-2-Nanometer Carbon Nanotubes*, Science **312**, 1034 (2006).

[6] L. R. Huang, E. C. Cox, R. H. Austin, and J. C. Sturm, *Continuous Particle Separation through Deterministic Lateral Displacement*, Science **304**, 987 (2004).

[7] M. P. MacDonald, G. C. Spalding, and K. Dholakia, *Microfluidic Sorting in an Optical Lattice*, Nature (London) **426**, 421 (2003).

[8] P. Hanggi and F. Marchesoni, *Artificial Brownian Motors: Controlling Transport on the Nanoscale*, Rev. Mod. Phys. **81**, 387 (2009).

[9] P. Reimann, *Brownian Motors: Noisy Transport Far from Equilibrium*, Phys. Rep. **361**, 57 (2002).

[10] M. Urbakh, J. Klafter, D. Gourdon, and J. Israelachvili, *The Nonlinear Nature of Friction*, Nature (London) **430**, 525 (2004).

[11] I. Szlufarska, M. Chandross, and R. W. Carpick, *Recent Advances in Single-Asperity Nanotribology*, J. Phys. D **41**, 123001 (2008).

[12] M. Schreier, P. Reimann, P. Hanggi, and E. Pollak, *Giant Enhancement of Diffusion and Particle Selection in Rocked Periodic Potentials*, Europhys. Lett. **44**, 416 (1998).

[13] H. Gang, A. Daffertshofer, and H. Haken, *Diffusion of Periodically Forced Brownian Particles Moving in Space-Periodic Potentials*, Phys. Rev. Lett. **76**, 4874 (1996).

[14] P. Romanczuk, F. Müller, and L. Schimansky-Geier, *Quasideterministic Transport of Brownian Particles in an Oscillating Periodic Potential*, Phys. Rev. E **81**, 061120 (2010).

[15] F. Mueller, P. Romanczuk, and L. Schimansky-Geier, *Synchronization and Transport in an Oscillating Periodic Potential*, Stoch. Dynam. **11**, 461 (2011).

[16] S. H. Lee and D. G. Grier, *Giant Colloidal Diffusivity on Corrugated Optical Vortices*, Phys. Rev. Lett. **96**, 190601 (2006).

[17] P. Tierno, P. Reimann, T. H. Johansen, and F. Sagues, *Giant Transversal Particle Diffusion in a Longitudinal Magnetic Ratchet*, Phys. Rev. Lett. **105**, 230602 (2010).

[18] D. C. Senft and G. Ehrlich, *Long Jumps in Surface Diffusion: One-Dimensional Migration of Isolated Adatoms*, Phys. Rev. Lett. **74**, 294 (1995).

[19] B. N. J. Persson, *Surface Resistivity—Theory and Applications*, Surf. Sci. **269–270**, 103 (1992).

[20] K. Lindenberg, A. M. Lacasta, J. M. Sancho, and A. H. Romero, *Transport and Diffusion on Crystalline Surfaces under External Forces*, New J. Phys. **7**, 29 (2005).

[21] Z. Tshiprut, A. E. Filippov, and M. Urbakh, *Tuning Diffusion and Friction in Microscopic Contacts by Mechanical Excitations*, Phys. Rev. Lett. **95**, 016101 (2005).

[22] J. Klafter and I. M. Sokolov, *First Steps in Random Walks: From Tools to Applications* (Oxford University Press, Oxford, England, 2011).

[23] T. Bohlein, J. Mikhael, and C. Bechinger, *Observation of Kinks and Antikinks in Colloidal Monolayers Driven across Ordered Surfaces*, Nat. Mater. **11**, 126 (2012).

[24] See Supplemental Material at http://link.aps.org/supplemental/10.1103/PhysRevX.5.031020 for parameter-free analytic model of diffusion, diffusion coefficients for adsorbates interacting through Lennard-Jones potentials, details of sample preparation, method for measuring cleaning effect, and effect of pushing near by slider edges.

[25] G. He and M. O. Robbins, *Simulations of the Kinetic Friction due to Adsorbed Surface Layers*, Tribol. Lett. **10**, 7 (2001).

[26] M. Cieplak, E. D. Smith, and M. O. Robbins, *Molecular-Origins of Friction—The Force on Adsorbed Layers*, Science **265**, 1209 (1994).

[27] Z. Liu, P. Boggild, J.-r. Yang, Y. Cheng, F. Grey, Y.-l. Liu, L. Wang, and Q.-s. Zheng, *A Graphite Nanoeraser*, Nanotechnology **22**, 265706 (2011).

[28] S. Redner, *A Guide to First-Passage Processes* (Cambridge University Press, Cambridge, England, 2001).

[29] A. Vanossi and O. M. Braun, *Driven Dynamics of Simplified Tribological Models*, J. Phys. Condens. Matter **19**, 305017 (2007).

[30] J. R. Yang, Z. Liu, F. Grey, Z. P. Xu, X. D. Li, Y. L. Liu, M. Urbakh, Y. Cheng, and Q. S. Zheng, *Observation of High-Speed Microscale Superlubricity in Graphite*, Phys. Rev. Lett. **110**, 255504 (2013).

[31] Z. Liu, J. Yang, F. Grey, J. Z. Liu, Y. Liu, Y. Wang, Y. Yang, Y. Cheng, and Q. Zheng, *Observation of Microscale Superlubricity in Graphite*, Phys. Rev. Lett. **108**, 205503 (2012).

[32] Q. Li, K. S. Kim, and A. Rydberg, *Lateral Force Calibration of an Atomic Force Microscope with a Diamagnetic Levitation Spring System*, Rev. Sci. Instrum. **77**, 065105 (2006).